The Signature of Inertial and Tidal Currents in Offshore Wave Records

JOHANNES GEMMRICH AND CHRIS GARRETT

University of Victoria, Victoria, British Columbia, Canada

(Manuscript received 2 March 2012, in final form 10 April 2012)

ABSTRACT

The roughness of the sea surface can be affected by strong currents. Here, long records of surface wave heights from buoy observations in the northeastern Pacific Ocean are examined. The data show the influence of tidal currents, but the first evidence of wave-height modulation (up to 20%) at a frequency that is slightly higher than the local inertial frequency is also found. This finding shows the effect on surface waves of near-inertial currents, which are typically the most energetic currents in the open ocean. The result has implications for wave forecasting but also provides valuable information on the frequency, strength, and intermittency of the associated near-inertial motions.

1. Introduction

The height of ocean surface waves is largely a function of wind speed, duration, and fetch (Holthuijsen 2007), and potential long-term trends in wave height might be a tool for monitoring climate change (Young et al. 2011). Ambient currents on various time scales can change the amplitude, direction, and frequency of ocean surface waves (Holthuijsen 2007). Regions with persistent strong currents, such as the Agulhas Current off the east coast of South Africa, are known as areas of extreme waves (Lavrenov 1998), and wave-height modulations of up to 50% observed in the shallow North Sea have been linked to tidal currents (Tolman 1990). In the open ocean, near-inertial motions, which propagate away from the surface and play a critical role in maintaining the ocean's abyssal stratification, can be dominant and may reach speeds of up to 0.5 m s^{-1} (Thomson et al. 1998; Park et al. 2005). However, their interaction with the surface wave field has not previously been reported.

Routine wave observations in the northeastern Pacific Ocean started in the 1970s. A network of operational wave buoys covers open-ocean and coastal locations off Canada and the United States. Standard meteorological data and wave-field parameters are reported hourly, and the time series are archived by the Integrated Science Data Management (http://www.meds-sdmm.dfo-mpo.gc.ca/isdm-gdsi/waves-vagues/index-eng.htm) and the National Data Buoy Center (http://www.ndbc.noaa.gov/) for Canadian and U.S. locations, respectively. Technical modifications of the buoy hardware and the data processing present challenges for long-term trend analyses but do not affect data quality over time scales of hours to days (Gemmrich et al. 2011). Here, we analyze wave buoy records from six locations in the open ocean, about 700 km offshore, and two near-shore locations (Fig. 1a) for the period of January 1988–December 2008. We focus on records of the significant wave height $H_s = 4\sigma$, where σ is the standard deviation of the surface elevation. The H_s values obtained by the buoys are based on an observation length of 34 min (Canadian buoys) and 20 or 40 min (U.S. buoys) and are reported hourly.

2. Spectral content of wave-height records

At the six offshore locations, the power spectra of H_s have a maximum at low frequencies (Fig. 1b), corresponding to fluctuations at the typical synoptic time scale of weather systems of several days (Fissel et al. 1976). In addition, all spectra show a small peak at the semidiurnal tidal frequency M_2 and a well-defined larger peak at a somewhat smaller frequency that is different for each location. In each spectrum, this peak occurs at a frequency that is approximately 2% higher than the local inertial frequency $f = 2\Omega \sin\phi$, where Ω is the rotation frequency of the earth and ϕ is the latitude

Corresponding author address: Johannes Gemmrich, Dept. of Physics and Astronomy, University of Victoria, P.O. Box 3055, Victoria BC V8W 3P6, Canada.
E-mail: gemmrich@uvic.ca

DOI: 10.1175/JPO-D-12-043.1

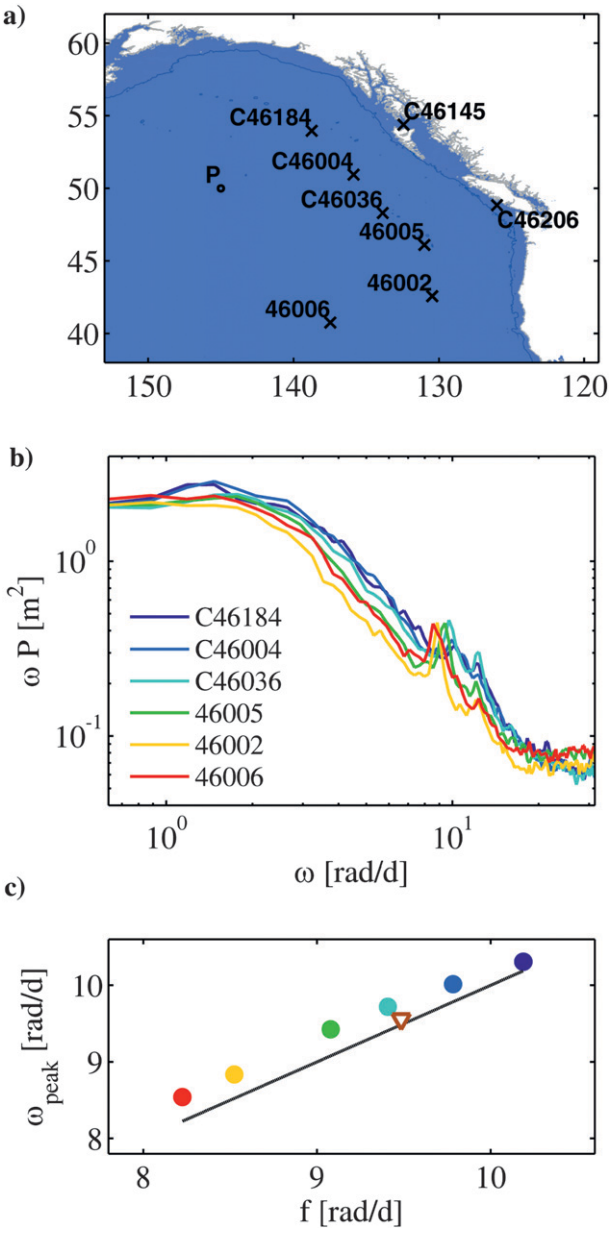

FIG. 1. Wave observations in the northeastern Pacific. (a) Position and name of stations. (b) Weighted power spectrum of significant wave heights, sampled at 1-h intervals. (c) Observed peak frequency in the inertial band ω_{peak} vs local inertial frequency f for the same stations as in (b) and for C46206 (brown open triangle).

(Fig. 1c). These peaks track the latitudinal dependence of f remarkably well.

Because there are no corresponding peaks in spectra of wind speed, these results suggest the influence of near-inertial surface currents. Moreover, the frequency shift (+2%) that we have found for the offshore wave records is consistent with that found for near-inertial currents observed at nearby station P (Alford et al. 2012). The currents are first generated by passing storm systems but are then subject to the Coriolis force and rotate in the anticyclonic direction at a rate corresponding to the local inertial frequency. Their frequency is shifted slightly higher because of the effect of a finite horizontal scale k^{-1}, where k is the horizontal wavenumber of the inertial wave. In regions with large-scale circulation, the frequency of near-inertial currents is also modified by the relative vorticity ζ of the large-scale background currents (Kunze 1985; D'Asaro 1995). Hence, the near-inertial current frequency ω is given by

$$\omega = (f^2 + c_n^2 k^2)^{1/2} + \zeta/2, \tag{1}$$

where c_n is the phase speed of the nth vertical mode. Near-inertial currents are typically dominated by the first mode, for which $c_1 \simeq 2.2$ m s^{-1} in the northeastern Pacific (Chelton et al. 1998). This implies that $k^{-1} \approx 100$ km if the frequency shift is 2% of f and ζ is small. The horizontal scale will be less if there is a mix of modes.

The spectrum of the H_s record from C46206, located in the open Pacific but just 25 km from shore, also shows a single sharp peak (Fig. 2a), although closer to the local inertial frequency (+0.8%; Fig. 1c). This result is a little surprising because it implies a very large horizontal scale k^{-1} for the near-inertial motions despite the proximity of the coast. It is likely that the anticyclonic shear of the local mean northward current, with $\zeta/2 \simeq -0.01f$, shifts the effective inertial frequency lower. Local vorticity may also account for the small frequency shift at C46184.

The other coastal station, C46145, is located roughly 100 km from the open Pacific in Dixon Entrance, a strait that is oriented east–west. It is approximately 200 km long but only 40 km wide and thus is not favorable for the generation of strong near-inertial currents. The power spectrum of the H_s time series shows no signal at the local inertial frequency, but there is a significant peak at the M_2 tidal frequency (Fig. 2b) and a much smaller second peak at its first harmonic, presumably as a consequence of wave interaction with the nearly rectilinear semidiurnal tidal currents of up to 0.6 m s^{-1} (Foreman 2004). The wind speed spectra at C46145 and C46206 (Fig. 2d) have a peak at the diurnal frequency but not at the semidiurnal or inertial frequencies, indicating that the relevant process for the wave modulation is the interaction between waves and currents rather than local wind forcing.

Although wave-height modulations by these periodic currents are clearly evident in the H_s power spectra, their contribution to the overall variance of the wave height is small. For a typical offshore station, C46036,

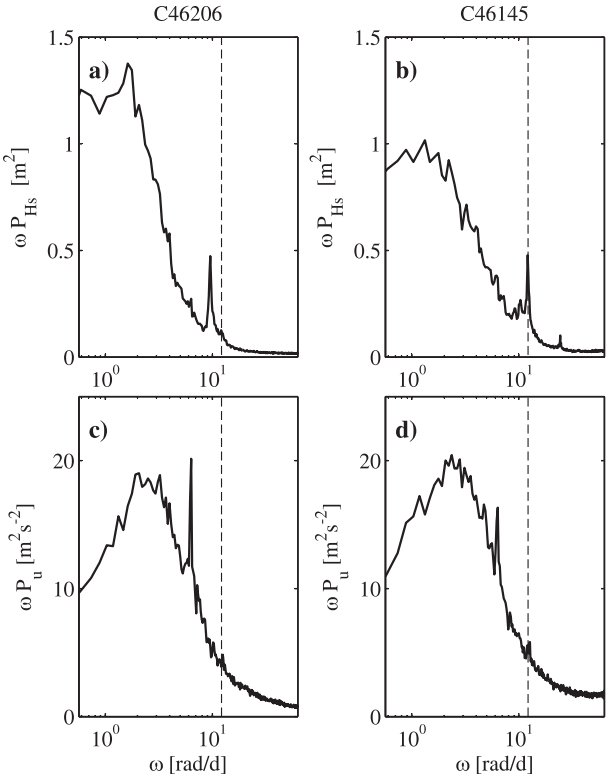

FIG. 2. Spectral content of wave-height and wind speed fluctuations at coastal stations. (a) Power spectrum of significant wave heights at location C46206 (La Perouse Bank, on the continental shelf facing the open ocean). (c) Corresponding spectrum of wind speed observations. (b),(d) As in (a),(c) but for location C46145 (Dixon Entrance, a tidal channel). The dashed lines depict the semidiurnal tidal frequency.

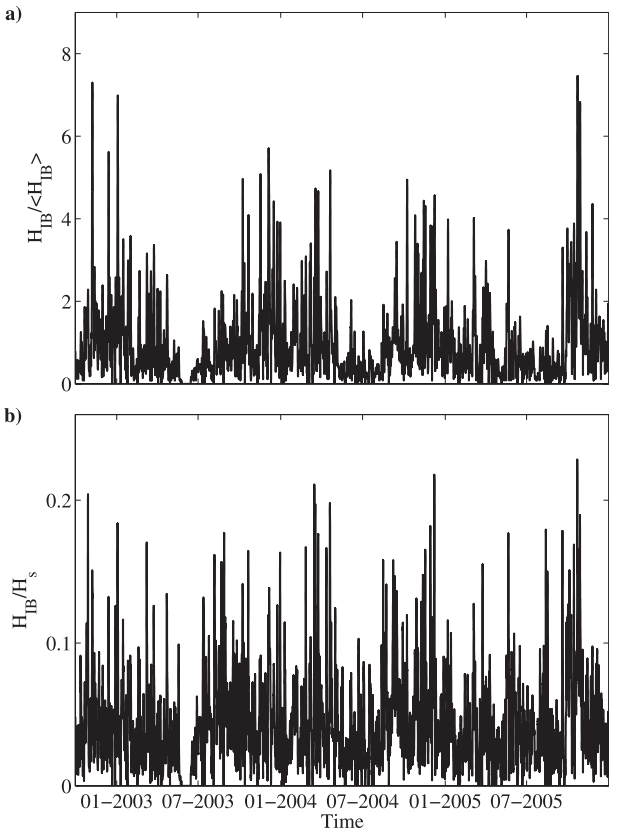

FIG. 3. Modulation of significant wave height within the internal wave band H_{IB} at station C46036, (a) normalized by its time-mean value $\langle H_{IB} \rangle$ and (b) relative to the total significant wave height H_s.

the extra variance in the near-inertial peak in the H_s spectrum, above that in a smooth underlying spectrum, is 0.003 m^2. The total H_s variance is made up of 1.7 m^2 from the integral of the underlying spectrum, corresponding to H_s fluctuations at all other frequencies, plus 8.3 m^2, which is the square of the mean significant wave height. Thus, the extra variance in the near-inertial peak in the H_s spectrum is just 0.03% of the background variance of H_s, and the average root-mean-square (rms) modulation of the wave height by near-inertial currents is just 2%. For a sinusoidal signal, the peak of the wave modulation is $2^{1/2}$ times the rms modulation, corresponding to a mean wave-height modulation of about 3%. This value is based on the average contribution of the inertial band throughout the entire record length. Because near-inertial currents occur only intermittently, the wave modulation by the currents is sometimes much larger than the average value.

To extract the time-varying signal within the inertial band, we used complex demodulation, centered at the local inertial frequency with a bandwidth of 2.1 rad day^{-1}. Figure 3a shows that wave-height modulation in the inertial band H_{IB} is largest during winter months and can frequently reach values of 4–6 times the average value $\langle H_{IB} \rangle$. The average contribution of wave-height modulation energy within the inertial band $\langle H_{IB}/H_s \rangle$ is about 4%, consistent with the estimate of 3% for $\langle H_{IB} \rangle / \langle H_s \rangle$ obtained from the power spectrum. However, this fraction frequently reaches values of up to 5 times the average value (Fig. 3b).

The open-ocean spectra shown in Fig. 1b also show a small peak at the tidal M_2 frequency. In principle the tidal currents are sufficiently predictable that a comparison with wave modulation in the time domain should be possible, but in practice uncertainties in global tidal models in this offshore region make this comparison unreliable. Furthermore, for the open-ocean locations the H_s variance in the tidal band is much less than that in the inertial band. There is no peak in the spectrum at the shelf location C46206 (Fig. 2a) at either the diurnal or semidiurnal tidal frequencies, possibly because the waves are generally propagating orthogonal to the (tidal) currents. The extra variance in the inertial peak

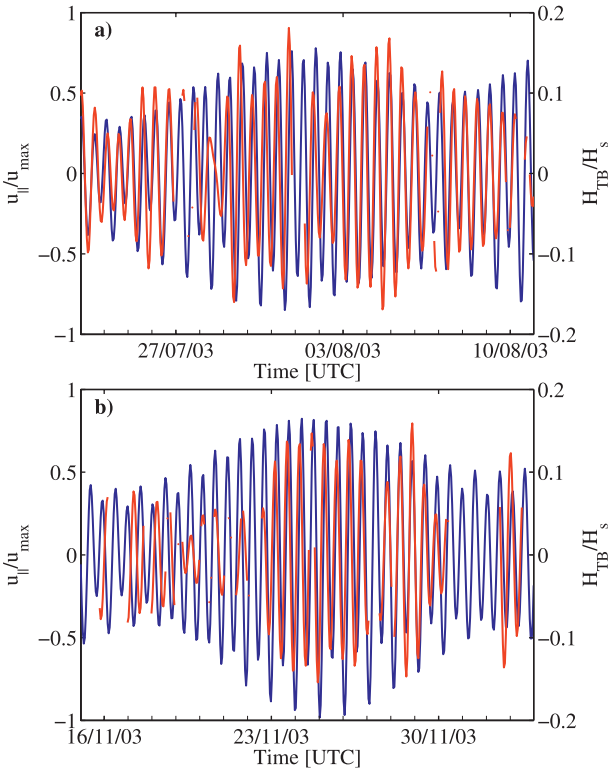

FIG. 4. Wave-height modulations by tidal currents at C46145 (central Dixon Entrance) during (a) low sea states and (b) higher sea states. Shown are fluctuations in significant wave height (red) and east–west component of the barotropic tidal current (blue). Wave-height data during periods of easterly winds are removed.

at C46206 is a fraction of 0.064% of the background (4.7 m^2 from mean H_s plus 1.2 m^2 from the variance), implying an rms modulation of the H_s of 3%. As for the offshore stations, a comparison in the time domain is not possible.

In the tidal channel (C46145), the extra variance in the semidiurnal peak in the wave spectrum, above that in a smooth underlying spectrum, is 0.003 m^2. This is a fraction of 0.09% of the background made up of the square 2.6 m^2 of the mean wave height plus the variance 0.9 m^2 of the underlying spectrum, indicating a mean wave-height modulation of about 4%. However, individual H_s fluctuations can be more significant.

3. Comparison in the time domain

Barotropic tidal currents in Dixon Entrance are predicted reliably enough that a time-domain comparison with significant wave heights at C46145 is possible. The time series of hourly H_s values is dominated by the passage of consecutive weather systems, but often a semidiurnal oscillation can be seen even in the raw data. To further highlight these oscillations, we extracted the wave-height signal in the tidal band H_{TB}, by filtering the H_s time series by complex demodulation, centered at the M_2 semidiurnal frequency with a 2.1 rad day^{-1} bandwidth. Figure 4 shows 19-day segments of modulations of significant wave height overlaid on the east–west component of the barotropic tidal currents u, normalized by the maximum barotropic tidal speed at this location $u_{max} = 0.63$ m s^{-1}. Wave-height fluctuations are normalized by the low-pass signal, obtained with a 13-point boxcar filter (13-h cutoff). No information on the wave direction is available, but it is likely that the wave field at C46145 is dominated by waves entering from the open Pacific. Therefore, we exclude periods with easterly (i.e., offshore) wind components, which might represent cases of mixed wave directions, from the following analysis. Thus, for all wave-height data included in the analysis, u/u_{max} is an estimate of the current component in the direction of the wave propagation.

The first example is taken from a period with relatively low sea state with max(H_s) $\approx$ 2 m and predominantly westerly wind direction (Fig. 4a). During the second segment, with max(H_s) $\approx$ 6 m, there are some more periods with waves that are potentially propagating westward, resulting in longer gaps in the wave-height fluctuation time series (Fig. 4b). However, in both examples wave-height modulations of 15%–20% exist, and in general stronger modulations are associated with stronger currents. Not every tidal cycle shows a modulation of the wave height. Therefore, when wave modulations occur, they are, on average, larger than the 3% average wave-height increase obtained from the increase in total variance (Fig. 2b).

Maybe even more remarkable than the magnitude of the wave modulation is the consistent phase relation, with increasing wave heights when wave propagation and currents are in the same direction and decreasing wave heights during the tidal phase of opposing currents. For each tidal cycle, we define wave-height modulations ΔH as the peak and trough values of H_{TB} and compare these with the current velocity at the time of the ΔH occurrences. Despite the wide scatter of individual data points, the average value of wave-height fluctuations for the entire data record with westerly wind directions clearly shows a positive correlation with the east–west component of the barotropic tidal current (Fig. 5), confirming the phase relation observed in the records from the shorter time series (Fig. 4).

4. Discussion

There are no observations or detailed model results of currents at the offshore buoy locations, and therefore

a direct comparison of the H_s modulation and the near-inertial current in the time domain is not possible. One possible mechanism for generating the observed wave-height modulations is that, for local wind-generated waves, it is the relative wind that matters (Fairall et al. 1996). This will be reduced if wind and current are in the same direction, leading to smaller waves, and vice versa. The significant wave height depends on many factors, but in wind-generated seas it generally scales with the wind speed U squared: $H_s \propto U^2/g$, with gravitational acceleration g (Holthuijsen 2007). Thus, a relative wind $U \pm u$, where u is the magnitude of the current speed, will be associated with wave-height fluctuations $\Delta H_s/H_s = \pm 2u/U$. For typical conditions, with $u = 0.2$ m s^{-1} and $U = 10$ m s^{-1}, this yields wave-height fluctuations of $\pm 4\%$. However, the wave climate in the northeastern Pacific is largely dominated by mature seas, and less than 5% of the data correspond to actively wind-forced waves with $U > c_p$, where c_p is the dominant phase speed of the waves.

Another possibility, for both swell and locally generated waves, is interaction of the waves with the currents. The theoretical framework for wave–current interactions is based on the conservation of wave action $A = E/\omega'$, where E is the wave energy density and ω' is the intrinsic wave frequency (Bretherton and Garrett 1968). Perhaps the most familiar wave–current interaction occurs for wave propagation from still water into an opposing current, as for waves propagating into an estuary, or waves propagating toward a tidal front (e.g., Baschek 2005). In that case, for weak currents the local wave energy density is increased by a factor of $(1 + 6u/c_0)^{-1}$ if u is the speed of the opposing current and c_0 is the wave phase speed in still water (Phillips 1977). For typical current speeds of 0.2 m s^{-1} and $c_0 = 10$ m s^{-1}, this translates into wave-height modulations of $\pm 6\%$.

Of course, the current field is not simply one dimensional, but significant changes in wave height are also expected as a consequence of refraction in more complicated current patterns. For example, major amplification may be experienced by waves propagating across a simple current jet, if the incident angle is shallow (Garrett 1976).

In the present situation, the current also varies with time. However, the role of time dependence is merely to change, with time, the current gradient into which the waves propagate. In the open northeastern Pacific, waves with a typical group speed of >5 m s^{-1} travel more than 60 km in the 3–4 h over which significant temporal changes in near-inertial currents occur, and this is comparable to the 100 km or less over which the currents change spatially.

Thus, both mechanisms, change of relative wind forcing and wave–current interaction, could result in noticeable modulations of the significant wave height, with the latter likely being more relevant in the swell-dominated wave climate of the northeastern Pacific. Further investigation is needed to establish why in Dixon Entrance (C46145) wave heights increase during periods of wave propagation in the direction of the barotropic tidal current and decrease in opposing currents. In particular, baroclinic tides may play a significant role in this area (B. Crawford 2012, personal communication).

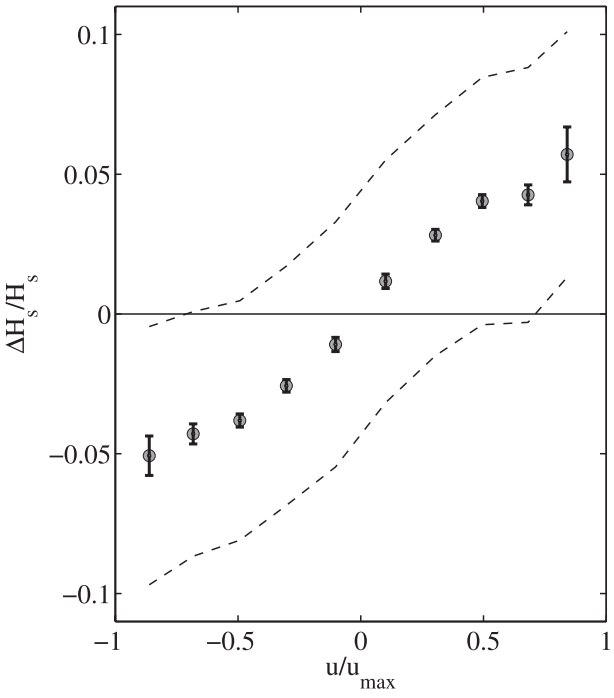

FIG. 5. Wave-height modulations by tidal currents, showing the average fluctuation of significant wave height as a function of the east–west component of barotropic tidal currents for station C46145 (central Dixon Entrance). The dashed lines represent 1 standard deviation of the spreading, and the vertical error bars represent the uncertainty of the average.

It would be useful if the occasional large modulation of H_s could be included in wave forecasts. Only a few operational wave forecast models include tidal currents as input parameters (WISE Group 2007), and the forecasts issued by Environment Canada for Dixon Entrance neglect wave–current interactions. None of the operational wave forecast models considers the effect of near-inertial currents, and doing so would require first that an operational model for these currents be developed. In the meantime, it makes sense to be aware of the possibility that significant modulation can occur. Opposing currents could also trigger nonlinear instabilities that lead to enhanced wave breaking and potentially more frequent rogue wave occurrences (Toffoli et al. 2011; Onorato et al. 2011).

Furthermore, near-inertial waves constitute the most energetic portion of the internal wave band and globally may contribute $O(25\%)$ of the energy flux required to maintain the abyssal stratification (Alford et al. 2012), thus playing a role comparable to that of internal tides in deep-ocean mixing. So far, observational data on near-surface inertial currents have tended to come from short records that do not permit reliable determination of the frequency blue shift, although this is an important factor affecting the energy flux from the surface into deeper waters. Long records from routine wave-height observations are widely available and may help to shed new light globally on the blue shift and on characteristics, such as the intermittency and strength, of near-inertial currents.

Acknowledgments. We thank Tom Farrar, Matthew Alford, and Jong-Jin Park for discussion. We gratefully acknowledge the support of the Government of Canada's Search and Rescue New Initiatives Fund and the Natural Sciences and Engineering Research Council.

REFERENCES

Alford, M. H., M. F. Cronin, and J. M. Klymak, 2012: Annual cycle and depth penetration of wind-generated near-inertial internal waves at Ocean Station Papa in the northeast Pacific. *J. Phys. Oceanogr.,* **42,** 889–909.

Baschek, B., 2005: Wave-current interaction in tidal fronts. *Rogue Waves: Proc. 14th 'Aha Huliko'a Hawaiian Winter Workshop,* Honolulu, HI, University of Hawaii at Manoa, 131–138.

Bretherton, F., and C. Garrett, 1968: Wavetrains in inhomogeneous moving media. *Proc. Roy. Soc. London,* **302A,** 529–554.

Chelton, D. B., R. A. deSzoeke, M. Schlax, K. El Naggar, and N. Siwertz, 1998: Geographical variability of the first baroclinic Rossby radius of deformation. *J. Phys. Oceanogr.,* **28,** 433–460.

D'Asaro, E., 1995: Upper-ocean inertial currents forced by a strong storm. Part III: Interaction of inertial currents and mesoscale eddies. *J. Phys. Oceanogr.,* **25,** 2953–2958.

Fairall, C., W. E. F. Bradley, D. P. Roger, J. B. Edson, and G. S. Young, 1996: Bulk parameterization of air-sea fluxes for Tropical Ocean–Global Atmosphere Coupled Ocean–Atmosphere Response Experiment. *J. Geophys. Res.,* **101C,** 3747–3764.

Fissel, D., S. Pond, and M. Miyake, 1976: Spectra of surface atmospheric quantities at ocean weathership P. *Atmosphere,* **14,** 77–97.

Foreman, M., 2004: Manual for tidal currents analysis and prediction. Institute of Ocean Sciences, Patricia Bay, Pacific Marine Science Rep. 78–6 (2004 revision of 1978 report), 65 pp.

Garrett, C., 1976: Generation of Langmuir circulations by surface waves—A feedback mechanism. *J. Mar. Res.,* **34,** 117–130.

Gemmrich, J., B. R. Thomas, and R. Bouchard, 2011: Observational changes and trends in northeast Pacific wave records. *Geophys. Res. Lett.,* **38,** L22601, doi:10.1029/2011GL049518.

Holthuijsen, L. H., 2007: *Waves in Oceanic and Coastal Waters.* Cambridge University Press, 387 pp.

Kunze, E., 1985: Near-inertial wave propagation in geostrophic shear. *J. Phys. Oceanogr.,* **15,** 544–565.

Lavrenov, I. V., 1998: The wave energy concentration at the Agulhas Current off South Africa. *Nat. Hazards,* **17,** 117–127.

Onorato, M., D. Proment, and A. Toffoli, 2011: Triggering rogue waves in opposing currents. *Phys. Rev. Lett.,* **107,** 184502, doi:10.1103/PhysRevLett.107.184502.

Park, J. J., K. Kim, and B. A. King, 2005: Global statistics of inertial motions. *Geophys. Res. Lett.,* **32,** L14612, doi:10.1029/2005GL023258.

Phillips, O. M., 1977: *Dynamics of the Upper Ocean.* Cambridge University Press, 336 pp.

Thomson, R. E., P. H. LeBlond, and A. Rabinovich, 1998: Satellite-tracked drifter measurements of inertial and semidiurnal currents in the northeast Pacific. *J. Geophys. Res.,* **103C,** 1039–1052.

Toffoli, A., and Coauthors, 2011: Occurrence of extreme waves in three-dimensional mechanically generated wave fields propagating over an oblique current. *Nat. Hazards Earth Syst. Sci.,* **11,** 895–903.

Tolman, H., 1990: The influence of unsteady depths and currents of tides on wind wave propagation in shelf seas. *J. Phys. Oceanogr.,* **20,** 1166–1174.

WISE Group, 2007: Wave modelling—The state of the art. *Prog. Oceanogr.,* **75,** 603–674.

Young, I. R., S. Zieger, and A. V. Babanin, 2011: Global trends in wind speed and wave height. *Science,* **332,** 451–455.